Chapter 8
Architecture and Assembly of the Bacterial Flagellar Motor Complex

Yusuke V. Morimoto and Tohru Minamino

Abstract One of the central systems responsible for bacterial motility is the flagellum. The bacterial flagellum is a macromolecular protein complex that is more than five times the cell length. Flagella-driven motility is coordinated via a chemosensory signal transduction pathway, and so bacterial cells sense changes in the environment and migrate towards more desirable locations. The flagellum of *Salmonella enterica* serovar Typhimurium is composed of a bi-directional rotary motor, a universal joint and a helical propeller. The flagellar motor, which structurally resembles an artificial motor, is embedded within the cell envelop and spins at several hundred revolutions per second. In contrast to an artificial motor, the energy utilized for high-speed flagellar motor rotation is the inward-directed proton flow through a transmembrane proton channel of the stator unit of the flagellar motor. The flagellar motor realizes efficient chemotaxis while performing high-speed movement by an ingenious directional switching mechanism of the motor rotation. To build the universal joint and helical propeller structures outside the cell body, the flagellar motor contains its own protein transporter called a type III protein export apparatus. In this chapter we summarize the structure and assembly of the *Salmonella* flagellar motor complex.

Keywords Bacterial flagellum · Flagellar assembly · Chemotaxis · Stator · Rotor · Torque generation · Type III protein export apparatus · Proton motive force

Y. V. Morimoto
Department of Physics and Information Technology, Faculty of Computer Science and Systems Engineering, Kyushu Institute of Technology, 680-4 Kawazu, Iizuka, Fukuoka 820-8502, Japan
e-mail: yvm001@bio.kyutech.ac.jp

T. Minamino (✉)
Graduate School of Frontier Biosciences, Osaka University, 1-3 Yamadaoka, Suita, Osaka 565-0871, Japan
e-mail: tohru@fbs.osaka-u.ac.jp

J. R. Harris and J. Marles-Wright (eds.), *Macromolecular Protein Complexes III: Structure and Function*, Subcellular Biochemistry 96,
https://doi.org/10.1007/978-3-030-58971-4_8

Introduction

The bacterial flagellum, which is a large filamentous assembly, is one of the organelles involved in motility in various environments such as liquids and solid surfaces. *Salmonella enterica* serovar Typhimurium (*Salmonella*) has several flagella on the cell body. Each flagellum is a supramolecular protein complex made of about 30 different proteins, and the copy number of each component protein varies from a few to tens of thousands. More than 60 proteins are involved in flagellar construction, force generation and chemotactic behavior in *Salmonella* (Table 8.1). The *Salmonella* flagellum is made of five distinct structural and functional parts: a base body, a hook, a junction, a filament and a filament cap (Fig. 8.1). The base body is embedded in the cellular membranes and works as a bi-directional rotary motor energized by the electrochemical potential difference of protons (H^+) across the cytoplasmic membrane (proton motive force, PMF). The hook, junction, filament and filament cap structures are located outside the bacterial cell body. The filament acts as a helical propeller to generate propulsion. The hook functions as a universal joint that smoothly transmits rotational force produced by the bi-directional rotary motor to the helical propeller. The junction connects the hook and filament. The filament cap supports the self-assembly of the filament protein, flagellin, into the long helical filament structure (Minamino and Imada 2015; Nakamura and Minamino 2019).

The *Salmonella* flagellar motor rotates in both counterclockwise (CCW) and clockwise (CW) directions. When all the flagellar motors rotate in CCW direction, long helical flagellar filaments form a bundle structure behind a cell body, due to bending flexibility of each hook structure. As a result, the flagellar bundle produces thrust enough to allow *Salmonella* cells to go straight. When one or more motors switch the rotational direction from CCW to CW, the bundle structure is partially disrupted, and so the cells stop swimming and change the swimming direction (Fig. 8.2a) (Morimoto and Minamino 2014). Each flagellar motor is placed under a control of the sensory signaling network, which modulates the switching frequency of flagellar motor rotation, and hence bacterial cells carry out chemotaxis by a biased random walk toward various chemicals, pH and temperature to move toward more suitable stimuli (Fig. 8.2b, c) (Berg 2003).

Methyl-accepting chemotaxis protein (MCP) is a transmembrane protein with a large cytoplasmic domain and senses temporal changes in environmental stimuli. The adapter protein CheW binds to the cytoplasmic domain of the MCP, allowing the CheA kinase to efficiently associate with the MCP. The cytoplasmic domain of MCP controls the autophosphorylation activity of the CheA kinase to generate the chemotaxis signal. A phosphorylated form of the CheA kinase transfers its phosphate group to CheY, which acts as the chemotaxis signaling protein. Phosphorylated CheY (CheY-P) binds to two cytoplasmic rotor component proteins, FliM and FliN, in the flagellar motor. As a result, the motor switches the direction of rotation from CCW to CW. The CheZ phosphatase accelerates the dephosphorylation of CheY-P to induce the dissociation of CheY from the motor to allow the motor to rotate CCW again. This chemotaxis signaling network adapts to changes in the concentration of

Table 8.1 Bacterial flagellar proteins in *Salmonella*

Protein	Function	Size (kD)
FliF	MS ring	61
FliG	C ring, torque generation, directional switch	37
FliM	C ring, directional switch	38
FliN	C ring, directional switch	15
FlhA	Type III export gate protein, energy transducer, protein export switch	75
FlhB	Type III export gate protein, protein export switch	42
FliH	Type III export apparatus, peripheral stalk	26
FliI	Type III export apparatus, ATPase	49
FliJ	Type III export apparatus, central stalk	17
FliO	Scaffolding protein for the assembly of the $FliP_5FliR_1$ complex	13
FliP	Type III export gate protein	27
FliQ	Type III export gate protein	10
FliR	Type III export gate protein	29
FlhE	Plug for a proton channel in a type III export apparatus	14
FlgN	Export chaperone specific for FlgK and FlgL	16
FliS	Export chaperone specific for FliC	15
FliT	Export chaperone specific for FliD	14
FliE	Basal body protein connecting the MS ring and the proximal rod	11
FlgB	Proximal rod	15
FlgC	Proximal rod	14
FlgF	Proximal rod	26
FlgG	Distal rod	28
FlgJ	Rod cap, Muramidase	34
FlgI	P ring	38
FlgA	Periplasmic chaperone for P ring assembly	24
FlgH	L ring	25
FlgD	Hook cap	24
FlgE	Hook	42
FliK	Hook-length control	42
FlgK	Hook-filament junction	59
FlgL	Hook-filament junction	34
FliD	Filament cap	50
FliC	Filament (H1 flagellin)	52
FljB	Filament (H2 flagellin)	53
FljA	Negative regulator of FliC expression	20
MotA	Stator, transmembrane proton channel	32

(continued)

Table 8.1 (continued)

Protein	Function	Size (kD)
MotB	Stator, transmembrane proton channel	34
FliL	Stator associated protein	17
FlhC	Master regulator for flagellar genes	22
FlhD	Master regulator for flagellar genes	13
FliA	Sigma factor/Chaperone specific for FlgM	27
FliZ	Positive regulator for flagellar gene expression	22
FlgM	Anti-sigma factor	11
CheZ	Chemotaxis protein	24
CheY	Chemotaxis protein	14
CheB	Chemotaxis protein	38
CheR	Chemotaxis protein	33
CheW	Chemotaxis protein	18
CheA	Chemotaxis protein	73
Tsr	Methyl-accepting chemotaxis protein	60
Tar	Methyl-accepting chemotaxis protein	60
Aer	Methyl-accepting chemotaxis protein	55

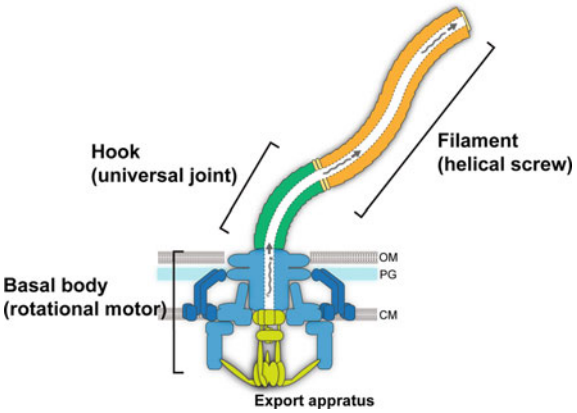

Fig. 8.1 Schematic diagram of the bacterial flagellar motor complex structure. The flagellum is composed of a filament, a hook and a basal body. Each building block synthesized in the cytoplasm is translocated via a type III protein export apparatus into the central channel of the growing axial structure. OM—outer membrane, PG—peptidoglycan layer, CM—cytoplasmic membrane

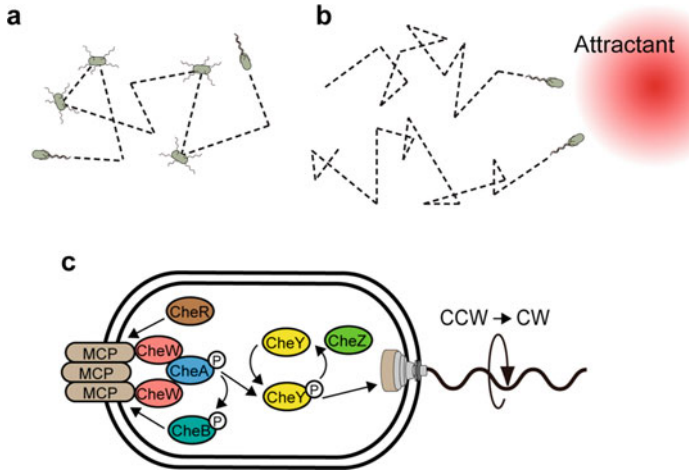

Fig. 8.2 **a** Swimming pattern of *Salmonella* cells. *Salmonella* cells undergoes continuous run-and-stop pattern, thereby showing random walk motions in liquids. When the flagellar motor rotates in counterclockwise (CCW) direction, *Salmonella* cells can go straight. In contrast, when the motor switches its rotational direction from CCW to counterclockwise (CW), the cells stop and change the swimming direction. **b** Biased random walk motion to attractants. *Salmonella* cells sense gradients of chemical attractants in the environments to move towards more favorable stimuli. **c** Schematic diagram of a sensory signaling transduction pathway responsible for chemotaxis. The *Salmonella* phosphorelay signal transduction network is formed by methyl-accepting chemotaxis protein (MCP), the CheW adopter protein, the CheA kinase, the CheY chemotaxis signaling protein, the CheZ phosphatase, the CheB methylesterase and the CheR methyltransferase. CheY-P binds to the switch complex of the flagellar motor to chnage the direction of flagellar motor rotation from CCW to CW

chemical stimuli over a wide dynamic range. CheB and CheR are involved in the adaption mechanism. CheR is the methyltransferase to induce the methylation of the cytoplasmic domain of the MCP to modulate the autophosphorylation activity of the CheA kinase. The CheA kinase also transfers the phosphate group to the CheB methylesterase to promote the demethylation of the MCP to reduce the probability of autophosphorylation of the CheA kinase (Fig. 8.2c) (Bi and Sourjik 2018).

The *Salmonella* flagellar motor consists of a rotor and about ten stator units placed around the rotor. The rotor is a macromolecular ring complex made of four flagellar proteins, FliF, FliG, FliM and FliN. The transmembrane MS ring is formed by FliF. FliG, FliM and FliN assemble into the C ring on the cytoplasmic surface of the MS ring in this order. The C ring also works as a directional switching device to switch between CCW and CW states of the flagellar motor. Each stator unit is composed of two integral membrane proteins, MotA and MotB, which form a proton channel complex to convert the energy of the proton flow through the channel into the rotational force (Minamino et al. 2018; Nakamura and Minamino 2019).

To construct the axial structure of the flagellum such as the hook and filament outside the cell body, the basal body has a type III protein export apparatus at its proximal end (Macnab 2003). The type III protein export apparatus is also a macromolecular protein complex consisting of a transmembrane export gate complex powered by PMF across the cytoplasmic membrane and an associated cytoplasmic ATPase ring complex and transports building blocks of the axial structure from the cytoplasm to the distal end of the nascent structure where each building block self-assembles into the axial structure. The export gate complex is located inside the central pore of the MS ring whereas the cytoplasmic ATPase ring complex associates with the C ring (Minamino 2014, 2018). In this chapter, we describe the structure and function of the bacterial flagellar motor complex in *Salmonella.*

Axial Structure

The *Salmonella* flagellum is composed of several basal body rings and an axial structure (Fig. 8.1). The axial structure is a helical, tubular structure consisting of six distinct structural parts: the proximal rod (FlgB, FlgC, FlgF), the distal rod (FlgG), the hook (FlgE), the junction (FlgK, FlgL), the filament (FliC, FljB), and the filament cap (FliD). The N- and C-terminal regions of each building block are disordered in solution but adopt a coiled coil in the inner core domain (D0) of the building block when they assemble into the axial structure (Fig. 8.3a) (Furukawa et al. 2002; Saijo-Hamano et al. 2004; Samatey et al. 2001). Hydrophobic interactions between the D0 domains of the building blocks are essential not only for the self-assembly of the axial structure but also for structural and mechanical stability of the entire tubular structure (Yonekura et al. 2003; Fujii et al. 2009; Maki-Yonekura et al. 2010; Saijo-Hamano et al. 2019). Except for the cap structure, which has five-fold rotational symmetry (Yonekura et al. 2000), the axial structure is a helical assembly composed of 11 protofilaments (Fig. 8.3b) (Yonekura et al. 2003; Fujii et al. 2009, 2017; Maki-Yonekura et al. 2010; Kato et al. 2019). The basic helical line that passes through all the subunits is called a 1-start helix, and there are approximately 11 subunits per two turns of the 1-start helix (Fig. 8.3b).

The rod is straight and rigid and acts as a drive shaft of the flagellar motor (Fujii et al. 2017). The hook is supercoiled and highly flexible in bending and functions as a universal joint (Samatey et al. 2004; Fujii et al. 2009; Kato et al. 2019). The filament is also supercoiled but rigid against bending and so functions as a helical propeller (Yonekura et al. 2003; Maki-Yonekura et al. 2010). The *Salmonella* filament normally adopts a left-handed supercoil to form a flagellar bundle structure behind a cell body for straight swimming and switches from the left-handed to right-handed supercoils when the flagellar motor switches the direction of rotation from CCW to CW (Calladine 1975, 1976; Maki-Yonekura et al. 2010). Since the rod and hook structurally look similar to each other, the hook is directly connected with the rod (Chevance et al. 2007; Fujii et al. 2017). In contrast, because there are structural and mechanical differences between the hook and filament, the junction is a cushioning

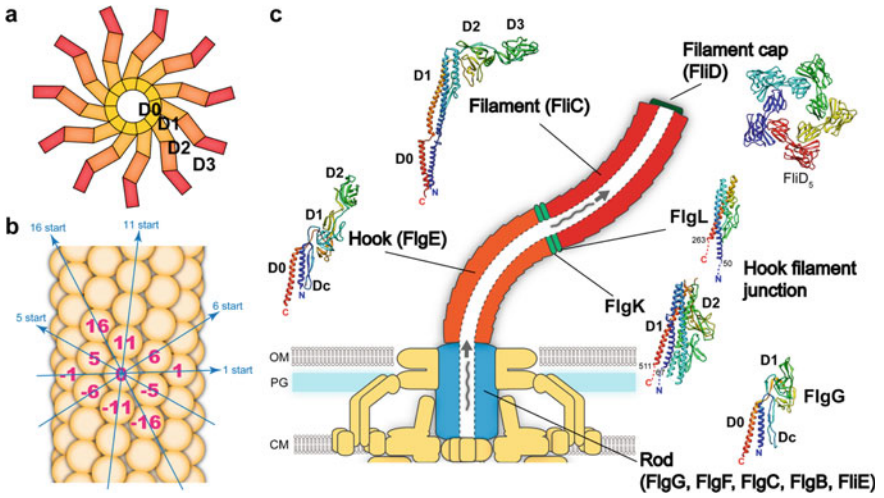

Fig. 8.3 Axial structure in the bacterial flagellar motor complex. **a** Schematic diagram of cross section of the flagellar filament. Flagellar filament protein is composed of domains D0, D1, D2 and D3. **b** Arrangement of building blocks in the flagellar axial structure composed of 11 protofilaments. Arrows show the helical lines. The 11-start helical line constitutes each protofilament. The numbers of the subunit starting from the subunit 0 along the 1-start helical line are shown. **c** Representative atomic structures of flagellar axial component proteins, FlgG (PDB ID, 6JZR), FlgE (PDB ID, 6KFK), FlgK (PDB ID, 2D4Y), FlgL (PDB ID, 2D4X), FliC (PDB ID, 1UCU) and FliD (PDB ID, 5H5T) derived from *Salmonella.* CM—cytoplasmic membrane, PG—peptidoglycan layer, OM—outer membrane

structure to connect them (Homma and Iino 1985). The filament cap promotes the self-assembly of flagellin subunits into the filament at the distal end (Ikeda et al. 1985, 1996; Yonekura et al. 2000).

Electron cryo-microscopy (cryo-EM) image analyses of the unusually elongated rod structure, namely polyrod, which is caused by the G65V substitution in the distal rod protein FlgG, have revealed that FlgG is composed of three domains, D0, Dc, and D1 from the inside to outside of the polyrod structure (Fig. 8.3c) (Fujii et al. 2017; Saijo-Hamano et al. 2019). Intermolecular interactions between FlgG subunits in the polyrod structure are very tight, and hence the rod is straight and rigid against bending to act as a drive shaft. Because FliE is an axial component protein of the basal body and interacts with the proximal rod protein FlgB, it is thought to form the most proximal part of the rod structure that is directly connected with the MS ring and/or the transmembrane export gate complex of the type III protein export apparatus (Minamino and Macnab 2000b; Minamino et al. 2000).

The hook is a short, curved structure composed of about 120 copies of the hook protein FlgE. FlgE consist of four domains, D0, Dc, D1 and D2, arranged from the inside to the outside of the hook structure (Fig. 8.3c) (Samatey et al. 2004; Fujii et al. 2009). Although the D0, Dc and D1 domains of FlgE are highly homologous to those of FlgG, there are structural and functional differences in the Dc domain

between FlgE and FlgG (Chevance et al. 2007; Fujii et al. 2017; Saijo-Hamano et al. 2019). The Dc domain of FlgG contains a FlgG-specific YQTIRQPGAQSSEQTTLP sequence (GSS), whereas FlgE does not. Insertion of the GSS into a corresponding region of the Dc domain of FlgE makes the hook straight and rigid in a way similar to the FlgG rod structure, suggesting that the GSS is important for the rigidity of the rod structure (Hiraoka et al. 2017). Axial packing interactions between a triangular loop of the D1 domain and the D2 domain in each protofilament of the hook structure are responsible for hook supercoiling (Samatey et al. 2004; Kato et al. 2019). However, a deletion of either a triangular loop of the D1 domain or domain D2 makes the hook straight but retains its bending flexibility, allowing the filaments to form a flagellar bundle behind a cell body (Sakai et al. 2018). Because there are gaps between FlgE subunits in the entire hook structure, these gaps are likely to contribute to bending flexibility of the hook (Fujii et al. 2009; Horvath et al. 2019; Kato et al. 2019; Shibata et al. 2019).

The filament is composed of more than 30,000 flagellin subunits and is a major target for antigens. *Salmonella* contains two flagellin genes *fliC* and *fljB* on the chromosomal DNA and expresses either FliC or FljB to form the filament on the cell surface. The alternate expression frequency of these two flagellin genes is about 10^{-3}–10^{-5} per cell per generation (Stocker 1949; Gillen and Hughes 1991), and such an autonomous switching changes the motility function as well as antigen response of *Salmonella* cells (Yamaguchi et al. 2020). The flagellin subunit is composed of four domains D0, D1, D2, and D3, arranged from the inner core to the outer surface of the filament (Fig. 8.3a, c) (Namba and Vonderviszt 1997). The D0 and D1 domains are responsible for the formation of the supercoiled form of the filament structure, and a β-hairpin in the D1 domain is thought to act as a structural switch that changes between left-handed and right-handed helical forms of the filament structure (Samatey et al. 2001). Because the D3 domain, which occupies the outermost part of the filament, is recognized as H antigens by host immune systems, the primary sequence of the D3 domain differs significantly between FliC and FljB. Interestingly, there are structural differences in the D3 domain between the FliC and FljB filaments, and such differences cause a significant difference in the helical propeller function of the filament under viscous conditions (Yamaguchi et al. 2020). The D3 domain of the flagellin molecule is dispensable for filament formation but contributes to thermal stability of the entire filament structure (Muskotal et al. 2010; Furukawa et al. 2016).

The filament growth occurs at the distal end of the growing filament structure (Minamino 2014). Purified flagellin subunits can self-assemble into a long helical filament in vitro (Asakura 1970). However, flagellin subunits require a filament cap formed by FliD to polymerize into the filament structure in vivo (Homma et al. 1984). If the FliD cap is missing, flagellin monomers cannot assemble into the filament and hence are secreted into the culture media. This suggests that the FliD cap prevents newly exported flagellin molecules from leaking into the culture media to ensure that each flagellin molecule has sufficient time to be incorporated into the filament. Interestingly, the stoichiometry of the filament cap structure is different among bacteria species. The *Salmonella* FliD cap has five-fold rotational symmetry (Fig. 8.3c), the *Escherichia coli* and *Pseudomonas aeruginosa* FliD caps have six-fold rotational

symmetry, and the *Serratia marcescens* and *Bdellovibrio bacteriovorus* FliD caps form a four-fold rotational symmetry structure (Yonekura et al. 2000; Maki-Yonekura et al. 2003; Postel et al. 2016; Ko et al. 2017; Song et al. 2017; Cho et al. 2019). These differences might be related to the structural diversity of the flagellin molecule.

Rotor

The *Salmonella* basal body has the C ring (FliG, FlM, FliN), the MS ring (FliF), the P ring (FlgI) and the L ring (FlgH), which are located in the cytoplasm, the cytoplasmic membrane, the peptidoglycan (PG) layer and the outer membrane, respectively (Fig. 8.4a). The MS ring and the C ring together form a rotor ring complex of the flagellar motor. The most proximal part of the rod is thought to be directly connected with the MS ring. The L and P rings together function as a bushing for the

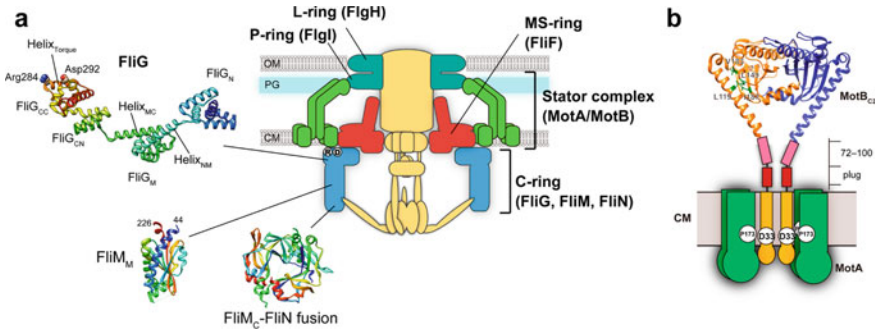

Fig. 8.4 Flagellar motor complex structure. **a** Cartoon of basal body rings. The basal body contains four ring structures named the C ring (FliG, FliM, FliN), the MS ring (FliF), the P ring (FlgI) and the L ring (FlgH). The MS ring and the C ring form the rotor ring complex of the flagellar motor. Crystal structures of *Aquifex aeolicus* FliG (PDB ID, 3HJL), *Thermotoga maritima* FliM middle domain ($FliM_M$) (PDB ID, 2HP7) and the *Salmonella* $FliM_C$-FliN fusion protein (PDB ID, 4YXB). FliG consists of three compactly folded domains, $FliG_N$, $FliG_M$ and $FliG_C$ that is able to be divided into two $FliG_{CN}$ and $FliG_{CC}$ subdomains and two linker helices, $Helix_{NM}$ connecting $FliG_N$ and $FliG_M$ and $Helix_{MC}$ connecting $FliG_M$ and $FliG_{CN}$. Two highly conserved charged residues, Arg284 (R) and Asp292 (D) in the torque helix of $FliG_{CC}$ are responsible for the interaction with the stator protein MotA. **b** Structure of the stator unit of the flagellar motor. The stator unit consists of four MotA and two MotB proteins and acts as a transmembrane proton channel to couple the proton flow to torque generation. Highly conserved Pro173 of MotA (P173) and Asp33 of MotB (D33) are directly involved in the proton translocation. The periplasmic domain of MotB ($MotB_C$) forms a homodimer and binds to the PG layer, allowing the MotA/MotB complex to act as a stator unit in the motor. A crystal structure of the $MotB_C$ dimer (PDB ID, 2ZVY) is shown. A linker region connecting MotB-TM and $MotB_C$ is dispensable for flagellar motor rotation but coordinates the proton channel activity of the MotA/MotB complex to stator assembly into the motor. The plug segment suppresses premature proton flow through the proton channel until the MotA/MotB complex become an active stator unit in the motor. CM—cytoplasmic membrane, PG—peptidoglycan layer, OM—outer membrane

distal rod structure, and the inner surface of the LP ring complex is likely to be very smooth for high-speed rotation of the rod as a drive shaft (Minamino et al. 2008).

FliF molecules with two transmembrane (TM) helices assemble into the MS ring in the cytoplasmic membrane. Over-expression of FliF alone from a pET-based plasmid vector results in the self-assembly of FliF subunits into the MS ring (Ueno et al. 1992). However, when FliF is expressed from the chromosomal DNA, FliF requires FliG for efficient formation of the MS ring in the cytoplasmic membrane (Morimoto et al. 2014). The N-terminal domain of FliG ($FliG_N$) binds to the C-terminal cytoplasmic domain of FliF (Kihara et al. 2000; Levenson et al. 2012). Intermolecular interactions between $FliG_N$ domains and between the middle ($FliG_M$) and C-terminal ($FliG_C$) domains of FliG are responsible for FliG ring formation on the cytoplasmic surface of the MS ring (Baker et al. 2016; Kim et al. 2017). The FliM/FliN complexes with a 1 FliM: 3 FliN stoichiometry bind to the FliG ring through an interaction between $FliG_M$ and FliM to form the C ring wall with 34-fold rotational symmetry (Paul et al. 2011; Vartanian et al. 2012; Lam et al. 2013). Because the torque helix in the C-terminal portion of $FliG_C$ ($FliG_{CC}$) is directly involved in the interaction with the stator protein MotA to generate the rotational force, $FliG_{CC}$ is believed to be located at the top of the C ring wall (Fig. 8.4a) (Zhou et al. 1998a). It has been reported that there is a symmetry mismatch between the MS and C rings (Suzuki et al. 2004), but recent high-resolution cryo-EM image analysis of the *Salmonella* MS ring have shown that the MS ring also has about 34-fold rotational symmetry (Johnson et al. 2020).

Many *Salmonella* mutants with altered motility have been isolated. Among motility mutants, mutations in FliG, FliM, and FliN confer a CCW switch bias phenotype or a CW switch bias phenotype even in the presence of the chemosensory signal transduction pathway. This suggests that these three C ring proteins are involved in directional switching of the flagellar motor (Yamaguchi et al. 1986). Genetic and biochemical analyses have revealed that the chemotaxis signaling protein CheY-P directly binds to the intrinsically disordered N-terminal region of FliM and the C-terminal domain of FliN in the C ring and promotes a highly cooperative conformational change in the FliG ring structure, allowing the motor to rotate in CW direction (Dyer et al. 2009; Sarkar et al. 2010). A conserved MFXF motif in a flexible hinge connecting the N-terminal portion of $FliG_C$ ($FliG_{CN}$) and $FliG_{CC}$ is thought to induce a 180° rotation of the torque helix of $FliG_{CC}$ relative to $FliG_{CN}$ when the motor switches the direction of rotation from CCW to CW (Lam et al. 2012; Miyanoiri et al. 2017). An in-frame deletion of three residues (Pro169–Ala170–Ala171) near the N-terminal portion of the linker helix connecting $FliG_M$ and $FliG_{CN}$ ($Helix_{MC}$) causes an extremely strong CW switch bias phenotype. The PAA deletion induces not only a distinct orientation of $Helix_{MC}$ relative to $FliG_M$ but also the rotation of $FliG_{CC}$ relative to $FliG_{CN}$, suggesting that $Helix_{MC}$ is postulated to act as a gear to coordinately switch the FliG ring structure between CCW and CW states (Minamino et al. 2011a; Kinoshita et al. 2018a, b). In addition to CheY-P, cyclic di-GMP (c-di-GMP), which is a second messenger molecule to induce biofilm formation, binds to YcgR to regulate chemotaxis through interactions of the c-di-GMP bound form of YcgR

with FliG and FliM in the C ring as well as MotA (Boehm et al. 2010; Fang and Gomelsky 2010; Paul et al. 2010).

The $FliM_1/FliN_3$ complex labeled with a fluorescent protein is visualized to exchange rapidly between the basal body and its cytoplasmic pool by high-resolution single molecule imaging techniques whereas neither FliF nor FliG does not, indicating that the C ring wall has a highly dynamic nature whereas both MS and FliG rings do not (Delalez et al. 2010; Fukuoka et al. 2010). The copy number of $FliM_1/FliN_3$ complex is estimated to be about 1.3 times higher in the CCW motor than in the CW motor (Delalez et al. 2014). Because the rapid turnover of the C ring wall depends on CheY-P, the directional switching of the flagellar motor seems to induce the dissociation of weakly bound $FliM_1/FliN_3$ complexes from the C ring wall (Lele et al. 2012; Branch et al. 2014; Delalez et al. 2014). The number of the $FliM_1/FliN_3$ complexes in the C ring increases with a decrease in the cytoplasmic concentration of CheY-P, suggesting that the motor adapts to changes in the steady-state level of CheY-P by tuning the copy number of the $FliM_1/FliN_3$ complex associated with the C ring wall (Lele et al. 2012; Branch et al. 2014; Delalez et al. 2014). However, because both purified CCW and CW motors have the C ring with 34-fold rotational symmetry (Sakai et al. 2019), it remains unknown how the FliG ring can accommodate additional $FliM_1/FliN_3$ complexes to the C ring.

Stator

MotA and MotB form a transmembrane proton channel that acts as a stator unit of the flagellar motor to couple the proton flow through the proton channel to torque generation (Fig. 8.4a) (Larsen et al. 1974; Manson et al. 1977; Ravid and Eisenbach 1984). MotA and MotB form a heterohexamer with a 4 MotA: 2 MotB stoichiometry and has two distinct proton channels (Fig. 8.4b) (Braun et al. 2004; Kojima and Blair 2004). MotA assembles into a homo-tetramer (Braun et al. 2004; Kim et al. 2008; Takekawa et al. 2016), and the MotB homo-dimer binds to the central pore of the MotA tetramer (Braun and Blair 2001). MotA has four TM helices (TM1–TM4), two short periplasmic loops between TM1 and TM2 and between TM3 and TM4, a relatively large cytoplasmic loop between TM2 and TM3 and a C-terminal cytoplasmic tail (Zhou et al. 1995). MotB has an N-terminal cytoplasmic tail, followed by a single TM helix and finally a large C-terminal periplasmic domain containing a peptidoglycan-binding (PGB) motif ($MotB_C$) (Kojima et al. 2009). The MotB-TM helix forms a proton channel with the TM3 and TM4 helices of MotA (Braun and Blair 2001; Braun et al. 2004). Highly conserved Asp33 of MotB and Pro173 of MotA, which are located in the proton channel, are involved in the proton flow through the channel (Zhou et al. 1998b; Braun et al. 1999; Kojima and Blair 2001; Che et al. 2008). The cytoplasmic loop of MotA contains highly conserved Arg90 and Glu98 residues that are responsible for the interaction with the torque helix of $FliG_{CC}$ (Zhou et al. 1998a). $MotB_C$ forms a dimer, and its dimerization is critical for efficient targeting and stable anchoring of the stator units to the PG layer. As a

result, the $MotA_4/MotB_2$ complex can become an active stator unit around a rotor (Kojima et al. 2009, 2018). Interestingly, site-specific disulfide bridge experiments have shown that $MotB_C$ is in relatively close proximity to the P ring of the basal body (Fig. 8.4a) (Hizukuri et al. 2010).

A flexible linker region of MotB (residues 51–100) connecting MotB-TM and the $MotB_C$ domain are dispensable for flagellar motor rotation (Fig. 8.4b) (Muramoto and Macnab 1998). Because an in-frame deletion of residues 53–66 of MotB considerably reduces cytoplasmic pH due to undesirable proton leakage through unassembled $MotA_4/MotB_2$ proton channel complex, residues 53–66 of MotB are postulated to form a plug segment to suppress the proton leakage through the proton channel until the $MotA_4/MotB_2$ complex is incorporated into a motor (Hosking et al. 2006; Morimoto et al. 2010a). Although the $MotA_4/MotB_2$ complex with a deletion of residues 51–100 of MotB is still functional, such a large deletion does not induce a considerable proton leakage through unassembled $MotA_4/MotB_2$ proton channel complexes (Muramoto and Macnab 1998). The MotB (L119P) substitution in the PGB domain of $MotB_C$ not only causes massive proton leakage though unassembled $MotA_4/MotB\ (\Delta 51–100)_2$ complexes (Kojima et al. 2009; Morimoto et al. 2010a) but also increase the binding affinity of the PGB domain for the PG layer (Kojima et al. 2018). The MotB (L119P) substitution induces an order-to-disorder transition of the N-terminal portion of the PGB domain (Kojima et al. 2018). Since a 5 nm extension of the PGB domain of MotB from the MotB-TM helix is required for the binding of the PGB domain to the PG layer (Kojima et al. 2008), such an order-to-disordered transition of the N-terminal portion of the PGB domain should occur when the $MotA_4/MotB_2$ complex encounters a rotor to become an active stator unit in the motor (Kojima et al. 2018). In agreement with this, the 5 nm extension process of the PGB domain of MotS derived from *Bacillus subtilis*, which is a MotB homologue, has been directly visualized using high-speed atomic force microscopy (Terahara et al. 2017a). Therefore, these observations suggest that the flexible linker region of MotB coordinates not only proper proton channel formation of the $MotA_4/MotB_2$ complex but also efficient and proper anchoring of the PGB domain to the PG layer.

Each stator complex binds to and dissociates from a rotor ring complex during torque generation by the flagellar motor, suggesting that the stator complex has a highly dynamic nature (Leake et al. 2006). The number of functionally active stators in the motor varies in response to changes in the environment, such as external load and external proton concentration (Fukuoka et al. 2009; Lele et al. 2013; Tipping et al. 2013; Che et al. 2014; Terahara et al. 2017b; Suzuki et al. 2019). For example, the maximum number of active stator units incorporated into the flagellar motor is about ten when the motor operates at high loads (Reid et al. 2006; Pourjaberi et al. 2017). In contrast, the stator number decreases from ten to a few with a decrease in external load (Yuan and Berg 2008; Nakamura et al. 2020). Thus, the flagellar motor autonomously controls the number of active stator units around the rotor in response to changes in external loads. It has been shown that an in-frame deletion of residues 72–100 of MotB results in much steeper decrease in the stator number with a decrease in the external load as compared to the wild-type motor (Castillo et al. 2013). This suggests that the linker region of MotB modulates the binding affinity of

the PGB domain for the PG layer in a load-dependent manner. Interestingly, certain point mutations in the cytoplasmic loop of MotA also change the load-sensitivity of the $MotA_4/MotB_2$ complex (Pourjaberi et al. 2017). Because the cytoplasmic loop of MotA directly binds to FliG to generate torque (Zhou et al. 1998a; Morimoto et al. 2010b; Morimoto et al. 2013), this cytoplasmic loop seems to act as a load sensor to coordinate the number of active stators incorporated into the motor in response to changes in external load. Recently, it has been shown that the localization efficiency of the $MotA_4/MotB_2$ complex is also increased by lowering extracellular pH, that is, increasing proton concentration, and that such an external pH-dependent localization pattern of the $MotA_4/MotB_2$ complex is not affected by the *motB(D33N)* mutation, which inhibits the proton flow through the $MotA_4/MotB_2$ proton channel complex (Suzuki et al. 2019). Since it has been reported that the PGB domain of MotS induces a disordered-to-order transition of the PGB domain in a Na^+-dependent manner to allow the $MotP_4/MotS_2$ complex to become an active stator unit in the *B. subtilis* flagellar motor (Terahara et al. 2017a), it is possible that the folding efficiency of the PGB domain of MotB depends on external pH values.

Type III Protein Export Apparatus

The assembly of the axial structure begins with the rod, followed by the hook, the junction, the filament cap in this order and finally the filament (Macnab 2003). For the self-assembly of each building block at the distal end of the growing structure, a type III protein export apparatus unfolds the building blocks synthesized in the cytoplasm and then transports them into the central channel of the growing structure (Minamino 2014; Minamino et al. 2020a). PMF across the cytoplasmic membrane and ATP are utilized as the energy sources to drive flagellar protein export by the type III protein export apparatus (Minamino and Namba 2008; Paul et al. 2008). The type III protein export apparatus is composed of a PMF-driven export gate complex consisting of five membrane proteins FlhA, FlhB, FliP, FliQ and FliR, and a cytoplasmic ATPase ring complex made of three cytoplasmic proteins, FliH, FliI and FliJ (Fig. 8.5) (Minamino 2014). These component proteins show sequence and functional similarities to those of the injectisome of pathogenic bacteria such as *Salmonella* spp, *Shigella* spp and *Yersinia* spp, which is involved in direct injection of effector proteins into eukaryotic host cells for bacterial infection (Galán et al. 2014). Furthermore, the overall structure of the cytoplasmic ATPase ring complex is similar to F-type and V-type rotary ATPase families, suggesting that the type III protein export apparatus of the flagellum and the injectisome share a common evolutionary origin with these rotary ATPase families (Imada et al. 2007, 2016; Ibuki et al. 2011). In addition, four cytoplasmic proteins, FlgN, FliA, FliS and FliT, function as flagellum-specific export chaperones to support the export of their cognate building blocks by the type III protein export apparatus (Table 8.1).

FliP, FliQ, FliR form a helical assembly with a 5 FliP: 4 FliQ: 1 FliR stoichiometry inside the central pore of the MS ring (Fig. 8.5) (Fabiani et al. 2017; Fukumura

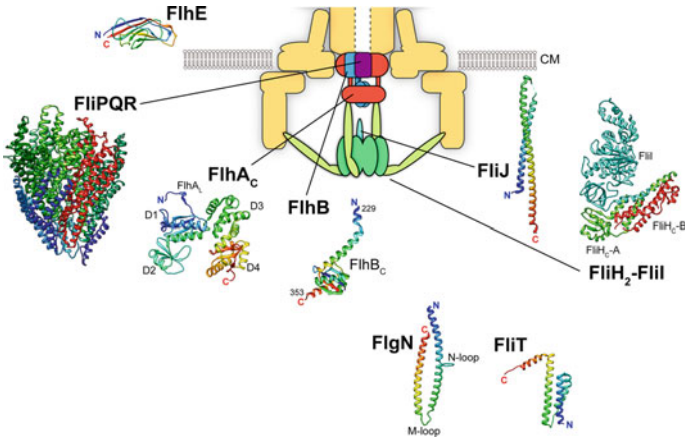

Fig. 8.5 Structures of the flagellar type III export apparatus component proteins. The type III protein export apparatus is composed of five transmembrane proteins, FlhA, FlhB, FliP, FliQ and FliR and three cytoplasmic protein FliH, FliI and FliJ. In addition, flagellar export chaperones such as FlgN and FliT interact with the type III protein export apparatus proteins to promote the export of their cognate building blocks. Crystal structures of the C-terminal cytoplasmic domain of *Salmonella* FlhA (FlhA$_C$) (PDB ID, 3A5I), the C-terminal cytoplasmic domain of *Salmonella* FlhB (FlhB$_C$) (PDB ID, 3B0Z), the *Salmonella* FliP/FliQ/FliR complex with a 5 FliP (green): 4 FliQ (blue): 1 FliR (red) stoichiometry (PDB ID, 6R69), *Salmonella* FlhE (PDB ID, 4QXL), *Salmonella* FliH$_2$FliI complex with a 2 FliH: 1 FliI stoichiometry (PDB ID, 5B0O), *Salmonella* FliJ (PDB ID, 3AJW) and the *Salmonella* FlgN (PDB ID, 5B3D) and FliT (PDB ID, 3A7M) export chaperones are shown. FlhA$_C$ consists of four compactly folded domains, D1, D2, D3 and D4 and a flexible linker connecting FlhA$_C$ and the N-terminal transmembrane region of FlhA. Hinge loops of the FlgN and FliT chaperones are responsible for helical rearrangements of these chaperone structure to modulate the binding affinity for their binding partners. CM—cytoplasmic membrane

et al. 2017; Kuhlen et al. 2018; Butan et al. 2019). The FliP$_5$/FliQ$_4$/FliR$_1$ complex is thought to be connected with the most proximal part of the rod to form a continuous protein channel inside the growing axial structure (Kuhlen et al. 2018). FlhA forms a homo-nonamer through intermolecular interactions between its C-terminal cytoplasmic domains (FlhA$_C$) (Abrusci et al. 2013; Kawamoto et al. 2013; Morimoto et al. 2014; Terahara et al. 2018) and acts as an energy transducer along with the cytoplasmic ATPase complex (Minamino et al. 2011b, 2016b; Erhardt et al. 2017). FlhA associates not only with the FliP$_5$/FliQ$_4$/FliR$_1$ helical structure but also with the MS ring (Kihara et al. 2001; Fukumura et al. 2017). A single copy of FlhB associates with FliP and FliR (Kuhlen et al. 2019). The assembly of the export gate complex begins with the formation of the FliP$_5$/FliR$_1$ complex with the help of the transmembrane protein FliO, followed by the assembly of FliQ and FlhB presumably in this order and finally the assembly of FlhA (Morimoto et al. 2014; Fabiani et al. 2017; Fukumura et al. 2017; Kuhlen et al. 2018). FlhA$_C$ and the C-terminal cytoplasmic domain of FlhB (FlhB$_C$) project into the central cavity of the C ring (Fig. 8.5) and form a docking platform for the cytoplasmic ATPase complex, flagellar export chaperones and building blocks (Bange et al. 2010; Minamino et al. 2010, 2012). These two

$FlhA_C$ and $FlhB_C$ domains mediate well-organized protein targeting and transport for efficient assembly of the axial structure with the help of the cytoplasmic ATPase complex and the molecular ruler protein FliK (Table 8.1) (Minamino and Macnab 2000a; Fraser et al. 2003; Hirano et al. 2009; Kinoshita et al. 2013; Minamino et al. 2016a, 2020b; Inoue et al. 2018, 2019).

FliI is a member of the Walker-type ATPase family (Fan and Macnab 1996) and forms a homo-hexamer to hydrolyze ATP at an interface between FliI subunits in a way similar to the $\alpha_3\beta_3$ hetero-hexameric ring complex of F_1-ATPase (Claret et al. 2003; Imada et al. 2007; Minamino et al. 2006). FliJ binds to the center of the FliI hexamer in a way similar to the γ subunit of the F_1-ATPase (Ibuki et al. 2011). The FliH dimer, which structurally looks similar to the peripheral stalk of the F_1-ATPase (Imada et al. 2016), binds to the N-terminal domain of each FliI subunit (Okabe et al. 2009) and anchors the $FliI_6FliJ$ ring complex to the flagellar base through interactions of the extreme N-terminal region of FliH with FliN and FlhA (Bai et al. 2014; Gonzalez-Pedrajo et al. 2006; Minamino et al. 2009; Hara et al. 2012). ATP hydrolysis by the FliI ATPase activates the PFM-driven export gate complex through an interaction between the FliJ stalk and FlhA, allowing the export gate complex to transport building blocks from the cytoplasm to the distal end of the growing structure in a PMF-dependent manner (Minamino et al. 2011b; Ibuki et al. 2013). The FliI ATPase shows rapid exchanges between the basal body and the cytoplasmic pool, suggesting that the cytoplasmic ATPase complex seems to be a dynamic structure (Bai et al. 2014).

When the cytoplasmic ATPase complex is missing, the transmembrane export gate complex utilizes sodium motive force across the cell membrane in addition to PFM (Minamino et al. 2016b). FlhA acts as the transmembrane ion channel of the export gate complex to conduct not only protons but also sodium ions (Minamino et al. 2016b). The transmembrane export gate complex functions as a protein/cation antiporter that couples the inward-directed cation flow through the FlhA channel to the outward-directed protein transport (Minamino et al. 2011b). The *flhE* gene forms an operon together with the *flhB* and *flhA* genes, and its gene product is secreted via the Sec translocon into the periplasm (Minamino et al. 1994). FlhE is postulated to act as a plug to prevent the FlhA ion channel from translocating large numbers of protons along an electrochemical difference of protons across the cytoplasmic membrane (Lee et al. 2015), but it remains unknown how it works. High-resolution local pH measurements around the type III protein export apparatus have shown that a loss of the ATPase ring complex increases the local pH inside the C ring, indicating ATP hydrolysis by the ATPase ring complex facilitates the proton channel activity of the FlhA channel coupled with flagellar protein export (Morimoto et al. 2016).

The FlgN, FliS and FliT chaperones not only suppresses premature aggregation and/or proteolysis of their cognate building blocks in the cytoplasm (Auvray et al. 2001; Bennett et al. 2001; Aldridge et al. 2003) but also facilitate their docking to the type III protein export apparatus (Thomas et al. 2004; Evans et al. 2006; Kinoshita et al. 2013). The FlgN, FliS and FliT chaperones adopt an α-helical structure (Fig. 8.5) (Evdokimov et al. 2003; Imada et al. 2010; Kinoshita et al. 2016), and the binding of their cognate building block to these chaperones induces helical rearrangements

of the chaperones through flexible hinge loops, allowing the building blocks to be efficiently transferred to the type III protein export apparatus, followed by efficient unfolding and the subsequent translocation of the building blocks by the PMF-driven export gate complex (Imada et al. 2010; Kinoshita et al. 2013, 2016; Furukawa et al. 2016).

Conclusions

Detailed domain structures of bacterial flagellar component proteins have been revealed at an atomic resolution by X-ray crystallography. In addition, cryo-EM image analyses of the bacterial flagellum have provided deep insights into the mechanical functions of the rod, the hook and the filament. Cryo-electron tomographic techniques have revealed the in situ structures of the transmembrane part of the basal body structure. However, while static structural knowledge is increasing, there are still many mysterious points that do not connect to dynamic functions of the bacterial flagellum. Biophysical and molecular genetic approaches combined with structural studies are required to more accurately investigate the dynamic mechanism of the flagellar motor complex.

Acknowledgements We acknowledge Profs. Keiichi Namba and Takuo Yasunaga for continuous support and encouragement. Our research is supported in part by the Japan Society for Promotion and Science.

References

Abrusci P, Vergara-Irigaray M, Johnson S, Beeby MD, Hendrixson DR, Roversi P, Friede ME, Deane JE, Jensen GJ, Tang CM, Lea SM (2013) Architecture of the major component of the type III secretion system export apparatus. Nat Struct Mol Biol 20(1):99–104. https://doi.org/10.1038/nsmb.2452

Aldridge P, Karlinsey J, Hughes KT (2003) The type III secretion chaperone FlgN regulates flagellar assembly via a negative feedback loop containing its chaperone substrates FlgK and FlgL. Mol Microbiol 49(5):1333–1345. https://doi.org/10.1046/j.1365-2958.2003.03637.x

Asakura S (1970) Polymerization of flagellin and polymorphism of flagella. Adv Biophys 1:99–155

Auvray F, Thomas J, Fraser GM, Hughes C (2001) Flagellin polymerisation control by a cytosolic export chaperone. J Mol Biol 308(2):221–229. https://doi.org/10.1006/jmbi.2001.4597

Bai F, Morimoto YV, Yoshimura SDJ, Hara N, Kami-Ike N, Namba K, Minamino T (2014) Assembly dynamics and the roles of FliI ATPase of the bacterial flagellar export apparatus. Sci Rep 4:6528. https://doi.org/10.1038/srep06528

Baker MA, Hynson RM, Ganuelas LA, Mohammadi NS, Liew CW, Rey AA, Duff AP, Whitten AE, Jeffries CM, Delalez NJ, Morimoto YV, Stock D, Armitage JP, Turberfield AJ, Namba K, Berry RM, Lee LK (2016) Domain-swap polymerization drives the self-assembly of the bacterial flagellar motor. Nat Struct Mol Biol 23(3):197–203. https://doi.org/10.1038/nsmb.3172

Bange G, Kummerer N, Engel C, Bozkurt G, Wild K, Sinning I (2010) FlhA provides the adaptor for coordinated delivery of late flagella building blocks to the type III secretion system. Proc Natl Acad Sci USA 107(25):11295–11300. https://doi.org/10.1073/pnas.1001383107

Bennett JC, Thomas J, Fraser GM, Hughes C (2001) Substrate complexes and domain organization of the *Salmonella* flagellar export chaperones FlgN and FliT. Mol Microbiol 39(3):781–791. https://doi.org/10.1046/j.1365-2958.2001.02268.x

Berg HC (2003) The rotary motor of bacterial flagella. Annu Rev Biochem 72:19–54. https://doi.org/10.1146/annurev.biochem.72.121801.161737

Bi S, Sourjik V (2018) Stimulus sensing and signal processing in bacterial chemotaxis. Curr Opin Microbiol 45:22–29. https://doi.org/10.1016/j.mib.2018.02.002

Boehm A, Kaiser M, Li H, Spangler C, Kasper CA, Ackermann M, Kaever V, Sourjik V, Roth V, Jenal U (2010) Second messenger-mediated adjustment of bacterial swimming velocity. Cell 141(1):107–116. https://doi.org/10.1016/j.cell.2010.01.018

Branch RW, Sayegh MN, Shen C, Nathan VSJ, Berg HC (2014) Adaptive remodelling by FliN in the bacterial rotary motor. J Mol Biol 426(19):3314–3324. https://doi.org/10.1016/j.jmb.2014.07.009

Braun TF, Blair DF (2001) Targeted disulfide cross-linking of the MotB protein of *Escherichia coli*: evidence for two H^+ channels in the stator complex. Biochemistry 40(43):13051–13059. https://doi.org/10.1021/bi011264g

Braun TF, Poulson S, Gully JB, Empey JC, Van Way S, Putnam A, Blair DF (1999) Function of proline residues of MotA in torque generation by the flagellar motor of *Escherichia coli*. J Bacteriol 181(11):3542–3551

Braun TF, Al-Mawsawi LQ, Kojima S, Blair DF (2004) Arrangement of core membrane segments in the MotA/MotB proton-channel complex of *Escherichia coli*. Biochemistry 43(1):35–45. https://doi.org/10.1021/bi035406d

Butan C, Lara-Tejero M, Li W, Liu J, Galan JE (2019) High-resolution view of the type III secretion export apparatus in situ reveals membrane remodeling and a secretion pathway. Proc Natl Acad Sci USA 116(49):24786–24795. https://doi.org/10.1073/pnas.1916331116

Calladine CR (1975) Construction of bacterial flagella. Nature 255(5504):121–124. https://doi.org/10.1038/255121a0

Calladine CR (1976) Design requirements for the construction of bacterial flagella. J Theor Biol 57(2):469–489. https://doi.org/10.1016/0022-5193(76)90016-3

Castillo DJ, Nakamura S, Morimoto YV, Che YS, Kami-Ike N, Kudo S, Minamino T, Namba K (2013) The C-terminal periplasmic domain of MotB is responsible for load-dependent control of the number of stators of the bacterial flagellar motor. Biophysics 9:173–181. https://doi.org/10.2142/biophysics.9.173

Che YS, Nakamura S, Kojima S, Kami-ike N, Namba K, Minamino T (2008) Suppressor analysis of the MotB(D33E) mutation to probe bacterial flagellar motor dynamics coupled with proton translocation. J Bacteriol 190(20):6660–6667. https://doi.org/10.1128/JB.00503-08

Che YS, Nakamura S, Morimoto YV, Kami-Ike N, Namba K, Minamino T (2014) Load-sensitive coupling of proton translocation and torque generation in the bacterial flagellar motor. Mol Microbiol 91(1):175–184. https://doi.org/10.1111/mmi.12453

Chevance FF, Takahashi N, Karlinsey JE, Gnerer J, Hirano T, Samudrala R, Aizawa S, Hughes KT (2007) The mechanism of outer membrane penetration by the eubacterial flagellum and implications for spirochete evolution. Genes Dev 21(18):2326–2335. https://doi.org/10.1101/gad.1571607

Cho SY, Song WS, Yoon SI (2019) Crystal structure of the flagellar cap protein FliD from *Bdellovibrio bacteriovorus*. Biochem Biophys Res Commun 519(3):652–658. https://doi.org/10.1016/j.bbrc.2019.09.024

Claret L, Calder SR, Higgins M, Hughes C (2003) Oligomerization and activation of the FliI ATPase central to bacterial flagellum assembly. Mol Microbiol 48(5):1349–1355. https://doi.org/10.1046/j.1365-2958.2003.03506.x

Delalez NJ, Wadhams GH, Rosser G, Xue Q, Brown MT, Dobbie IM, Berry RM, Leake MC, Armitage JP (2010) Signal-dependent turnover of the bacterial flagellar switch protein FliM. Proc Natl Acad Sci USA 107(25):11347–11351. https://doi.org/10.1073/pnas.1000284107

Delalez NJ, Berry RM, Armitage JP (2014) Stoichiometry and turnover of the bacterial flagellar switch protein FliN. mBio 5(4):e01216–01214. https://doi.org/10.1128/mBio.01216-14

Dyer CM, Vartanian AS, Zhou H, Dahlquist FW (2009) A molecular mechanism of bacterial flagellar motor switching. J Mol Biol 388(1):71–84. https://doi.org/10.1016/j.jmb.2009.02.004

Erhardt M, Wheatley P, Kim EA, Hirano T, Zhang Y, Sarkar MK, Hughes KT, Blair DF (2017) Mechanism of type-III protein secretion: regulation of FlhA conformation by a functionally critical charged-residue cluster. Mol Microbiol 104(2):234–249. https://doi.org/10.1111/mmi.13623

Evans LD, Stafford GP, Ahmed S, Fraser GM, Hughes C (2006) An escort mechanism for cycling of export chaperones during flagellum assembly. Proc Natl Acad Sci USA 103(46):17474–17479. https://doi.org/10.1073/pnas.0605197103

Evdokimov AG, Phan J, Tropea JE, Routzahn KM, Peters HK, Pokross M, Waugh DS (2003) Similar modes of polypeptide recognition by export chaperones in flagellar biosynthesis and type III secretion. Nat Struct Biol 10(10):789–793. https://doi.org/10.1038/nsb982

Fabiani FD, Renault TT, Peters B, Dietsche T, Galvez EJC, Guse A, Freier K, Charpentier E, Strowig T, Franz-Wachtel M, Macek B, Wagner S, Hensel M, Erhardt M (2017) A flagellum-specific chaperone facilitates assembly of the core type III export apparatus of the bacterial flagellum. PLoS Biol 15(8):e2002267. https://doi.org/10.1371/journal.pbio.2002267

Fan F, Macnab RM (1996) Enzymatic characterization of FliI—an ATPase involved in flagellar assembly in *Salmonella* typhimurium. J Biol Chem 271(50):31981–31988

Fang X, Gomelsky M (2010) A post-translational, c-di-GMP-dependent mechanism regulating flagellar motility. Mol Microbiol 76(5):1295–1305. https://doi.org/10.1111/j.1365-2958.2010.07179.x

Fraser GM, Hirano T, Ferris HU, Devgan LL, Kihara M, Macnab RM (2003) Substrate specificity of type III flagellar protein export in *Salmonella* is controlled by subdomain interactions in FlhB. Mol Microbiol 48(4):1043–1057. https://doi.org/10.1046/j.1365-2958.2003.03487.x

Fujii T, Kato T, Namba K (2009) Specific arrangement of alpha-helical coiled coils in the core domain of the bacterial flagellar hook for the universal joint function. Structure 17(11):1485–1493. https://doi.org/10.1016/j.str.2009.08.017

Fujii T, Kato T, Hiraoka KD, Miyata T, Minamino T, Chevance FF, Hughes KT, Namba K (2017) Identical folds used for distinct mechanical functions of the bacterial flagellar rod and hook. Nat Commun 8:14276. https://doi.org/10.1038/ncomms14276

Fukumura T, Makino F, Dietsche T, Kinoshita M, Kato T, Wagner S, Namba K, Imada K, Minamino T (2017) Assembly and stoichiometry of the core structure of the bacterial flagellar type III export gate complex. PLoS Biol 15(8):e2002281. https://doi.org/10.1371/journal.pbio.2002281

Fukuoka H, Wada T, Kojima S, Ishijima A, Homma M (2009) Sodium-dependent dynamic assembly of membrane complexes in sodium-driven flagellar motors. Mol Microbiol 71(4):825–835. https://doi.org/10.1111/j.1365-2958.2008.06569.x

Fukuoka H, Inoue Y, Terasawa S, Takahashi H, Ishijima A (2010) Exchange of rotor components in functioning bacterial flagellar motor. Biochem Biophys Res Commun 394(1):130–135. https://doi.org/10.1016/j.bbrc.2010.02.129

Furukawa Y, Imada K, Vonderviszt F, Matsunami H, Sano K, Kutsukake K, Namba K (2002) Interactions between bacterial flagellar axial proteins in their monomeric state in solution. J Mol Biol 318(3):889–900. https://doi.org/10.1016/S0022-2836(02)00139-0

Furukawa Y, Inoue Y, Sakaguchi A, Mori Y, Fukumura T, Miyata T, Namba K, Minamino T (2016) Structural stability of flagellin subunit affects the rate of flagellin export in the absence of FliS chaperone. Mol Microbiol 102(3):405–416. https://doi.org/10.1111/mmi.13469

Galán JE, Lara-Tejero M, Marlovits TC, Wagner S (2014) Bacterial type III secretion systems: specialized nanomachines for protein delivery into target cells. Annu Rev Microbiol 68:415–438. https://doi.org/10.1146/annurev-micro-092412-155725

Gillen KL, Hughes KT (1991) Negative regulatory loci coupling flagellin synthesis to flagellar assembly in *Salmonella typhimurium*. J Bacteriol 173(7):2301–2310. https://doi.org/10.1128/jb.173.7.2301-2310.1991

Gonzalez-Pedrajo B, Minamino T, Kihara M, Namba K (2006) Interactions between C ring proteins and export apparatus components: a possible mechanism for facilitating type III protein export. Mol Microbiol 60(4):984–998. https://doi.org/10.1016/j.1365-2958.2006.05149.x

Hara N, Morimoto YV, Kawamoto A, Namba K, Minamino T (2012) Interaction of the extreme N-terminal region of FliH with FlhA is required for efficient bacterial flagellar protein export. J Bacteriol 194(19):5353–5360. https://doi.org/10.1128/JB.01028-12

Hirano T, Mizuno S, Aizawa S, Hughes KT (2009) Mutations in *flk*, *flgG*, *flhA*, and *flhE* that affect the flagellar type III secretion specificity switch in *Salmonella enterica*. J Bacteriol 191(12):3938–3949. https://doi.org/10.1128/JB.01811-08

Hiraoka KD, Morimoto YV, Inoue Y, Fujii T, Miyata T, Makino F, Minamino T, Namba K (2017) Straight and rigid flagellar hook made by insertion of the FlgG specific sequence into FlgE. Sci Rep 7:46723. https://doi.org/10.1038/srep46723

Hizukuri Y, Kojima S, Homma M (2010) Disulphide cross-linking between the stator and the bearing components in the bacterial flagellar motor. J Biochem 148(3):309–318. https://doi.org/10.1093/jb/mvq067

Homma M, Iino T (1985) Locations of hook-associated proteins in flagellar structures of *Salmonella typhimurium*. J Bacteriol 162(1):183–189

Homma M, Fujita H, Yamaguchi S, Iino T (1984) Excretion of unassembled flagellin by *Salmonella typhimurium* mutants deficient in hook-associated proteins. J Bacteriol 159(3):1056–1059

Horvath P, Kato T, Miyata T, Namba K (2019) Structure of *Salmonella* flagellar hook reveals intermolecular domain interactions for the universal joint function. Biomolecules 9(9):462. https://doi.org/10.3390/biom9090462

Hosking ER, Vogt C, Bakker EP, Manson MD (2006) The *Escherichia coli* MotAB proton channel unplugged. J Mol Biol 364(5):921–937. https://doi.org/10.1016/j.jmb.2006.09.035

Ibuki T, Imada K, Minamino T, Kato T, Miyata T, Namba K (2011) Common architecture of the flagellar type III protein export apparatus and F- and V-type ATPases. Nat Struct Mol Biol 18(3):277–282. https://doi.org/10.1038/nsmb.1977

Ibuki T, Uchida Y, Hironaka Y, Namba K, Imada K, Minamino T (2013) Interaction between FliJ and FlhA, components of the bacterial flagellar type III export apparatus. J Bacteriol 195(3):466–473. https://doi.org/10.1128/JB.01711-12

Ikeda T, Asakura S, Kamiya R (1985) "Cap" on the tip of *Salmonella* flagella. J Mol Biol 184(4):735–737. https://doi.org/10.1016/0022-2836(85)90317-1

Ikeda T, Oosawa K, Hotani H (1996) Self-assembly of the filament capping protein, FliD, of bacterial flagella into an annular structure. J Mol Biol 259(4):679–686. https://doi.org/10.1006/jmbi.1996.0349

Imada K, Minamino T, Tahara A, Namba K (2007) Structural similarity between the flagellar type III ATPase FliI and F1-ATPase subunits. Proc Natl Acad Sci USA 104(2):485–490. https://doi.org/10.1073/pnas.0608090104

Imada K, Minamino T, Kinoshita M, Furukawa Y, Namba K (2010) Structural insight into the regulatory mechanisms of interactions of the flagellar type III chaperone FliT with its binding partners. Proc Natl Acad Sci USA 107(19):8812–8817. https://doi.org/10.1073/pnas.1001866107

Imada K, Minamino T, Uchida Y, Kinoshita M, Namba K (2016) Insight into the flagella type III export revealed by the complex structure of the type III ATPase and its regulator. Proc Natl Acad Sci USA 113(13):3633–3638. https://doi.org/10.1073/pnas.1524025113

Inoue Y, Morimoto YV, Namba K, Minamino T (2018) Novel insights into the mechanism of well-ordered assembly of bacterial flagellar proteins in *Salmonella*. Sci Rep 8(1):1787. https://doi.org/10.1038/s41598-018-20209-3

Inoue Y, Ogawa Y, Kinoshita M, Terahara N, Shimada M, Kodera N, Ando T, Namba K, Kitao A, Imada K, Minamino T (2019) Structural insights into the substrate specificity switch mechanism

of the type III protein export apparatus. Structure 27(6):965-976.e6. https://doi.org/10.1016/j.str.2019.03.017

Johnson S, Fong YH, Deme J, Furlong E, Kuhlen L, Lea SM (2020) Symmetry mismatch in the MS-ring of the bacterial flagellar rotor explains the structural coordination of secretion and rotation. Nat Microbiol 5(7): 966–975. https://doi.org/10.1038/s41564-020-0703-3.

Kato T, Makino F, Miyata T, Horvath P, Namba K (2019) Structure of the native supercoiled flagellar hook as a universal joint. Nat Commun 10(1):5295. https://doi.org/10.1038/s41467-019-13252-9

Kawamoto A, Morimoto YV, Miyata T, Minamino T, Hughes KT, Kato T, Namba K (2013) Common and distinct structural features of *Salmonella* injectisome and flagellar basal body. Sci Rep 3:3369. https://doi.org/10.1038/srep03369

Kihara M, Miller GU, Macnab RM (2000) Deletion analysis of the flagellar switch protein FliG of *Salmonella*. J Bacteriol 182(11):3022–3028. https://doi.org/10.1128/jb.182.11.3022-3028.2000

Kihara M, Minamino T, Yamaguchi S, Macnab RM (2001) Intergenic suppression between the flagellar MS ring protein FliF of *Salmonella* and FlhA, a membrane component of its export apparatus. J Bacteriol 183(5):1655–1662. https://doi.org/10.1128/jb.183.5.1655-1662.2001

Kim EA, Price-Carter M, Carlquist WC, Blair DF (2008) Membrane segment organization in the stator complex of the flagellar motor: implications for proton flow and proton-induced conformational change. Biochemistry 47(43):11332–11339. https://doi.org/10.1021/bi801347a

Kim EA, Panushka J, Meyer T, Carlisle R, Baker S, Ide N, Lynch M, Crane BR, Blair DF (2017) Architecture of the flagellar switch complex of *Escherichia coli*: conformational plasticity of FliG and implications for adaptive remodeling. J Mol Biol 429(9):1305–1320. https://doi.org/10.1016/j.jmb.2017.02.014

Kinoshita M, Hara N, Imada K, Namba K, Minamino T (2013) Interactions of bacterial flagellar chaperone-substrate complexes with FlhA contribute to co-ordinating assembly of the flagellar filament. Mol Microbiol 90(6):1249–1261. https://doi.org/10.1111/mmi.12430

Kinoshita M, Nakanishi Y, Furukawa Y, Namba K, Imada K, Minamino T (2016) Rearrangements of alpha-helical structures of FlgN chaperone control the binding affinity for its cognate substrates during flagellar type III export. Mol Microbiol 101(4):656–670. https://doi.org/10.1111/mmi.13415

Kinoshita M, Furukawa Y, Uchiyama S, Imada K, Namba K, Minamino T (2018a) Insight into adaptive remodeling of the rotor ring complex of the bacterial flagellar motor. Biochem Biophys Res Commun 496(1):12–17. https://doi.org/10.1016/j.bbrc.2017.12.118

Kinoshita M, Namba K, Minamino T (2018b) Effect of a clockwise-locked deletion in FliG on the FliG ring structure of the bacterial flagellar motor. Genes Cells 23(3):241–247. https://doi.org/10.1111/gtc.12565

Kojima S, Blair DF (2001) Conformational change in the stator of the bacterial flagellar motor. Biochemistry 40(43):13041–13050. https://doi.org/10.1021/bi011263o

Kojima S, Blair DF (2004) Solubilization and purification of the MotA/MotB complex of *Escherichia coli*. Biochemistry 43(1):26–34. https://doi.org/10.1021/bi0354051

Kojima S, Furukawa Y, Matsunami H, Minamino T, Namba K (2008) Characterization of the periplasmic domain of MotB and implications for its role in the stator assembly of the bacterial flagellar motor. J Bacteriol 190(9):3314–3322. https://doi.org/10.1128/JB.01710-07

Kojima S, Imada K, Sakuma M, Sudo Y, Kojima C, Minamino T, Homma M, Namba K (2009) Stator assembly and activation mechanism of the flagellar motor by the periplasmic region of MotB. Mol Microbiol 73(4):710–718. https://doi.org/10.1111/j.1365-2958.2009.06802.x

Kojima S, Takao M, Almira G, Kawahara I, Sakuma M, Homma M, Kojima C, Imada K (2018) The helix rearrangement in the periplasmic domain of the flagellar stator B subunit activates peptidoglycan binding and ion influx. Structure 26(4):590–598, e595. https://doi.org/10.1016/j.str.2018.02.016

Ko W, Lim S, Lee W, Kim Y, Berg HC, Peskin CS (2017) Modeling polymorphic transformation of rotating bacterial flagella in a viscous fluid. Phys Rev E 95(6–1):063106. https://doi.org/10.1103/PhysRevE.95.063106

Kuhlen L, Abrusci P, Johnson S, Gault J, Deme J, Caesar J, Dietsche T, Mebrhatu MT, Ganief T, Macek B, Wagner S, Robinson CV, Lea SM (2018) Structure of the core of the type III secretion system export apparatus. Nat Struct Mol Biol 25(7):583–590. https://doi.org/10.1038/s41594-018-0086-9

Kuhlen L, Johnson S, Zeitler A, Bäurle S, Deme JC, Debo R, Fisher J, Wagner S, Lea SM (2019) The flagellar substrate specificity switch protein FlhB assembles onto the extra-membrane export gate to regulate type three secretion. bioRxiv:686782. https://doi.org/10.1101/686782

Lam KH, Ip WS, Lam YW, Chan SO, Ling TKW, Au SWN (2012) Multiple conformations of the FliG C-terminal domain provide insight into flagellar motor switching. Structure 20(2):315–325. https://doi.org/10.1016/j.str.2011.11.020

Lam KH, Lam WW, Wong JY, Chan LC, Kotaka M, Ling TK, Jin DY, Ottemann KM, Au SW (2013) Structural basis of FliG-FliM interaction in *Helicobacter pylori*. Mol Microbiol 88(4):798–812. https://doi.org/10.1111/mmi.12222

Larsen SH, Adler J, Gargus JJ, Hogg RW (1974) Chemomechanical coupling without ATP: the source of energy for motility and chemotaxis in bacteria. Proc Natl Acad Sci USA 71(4):1239–1243. https://doi.org/10.1073/pnas.71.4.1239

Leake MC, Chandler JH, Wadhams GH, Bai F, Berry RM, Armitage JP (2006) Stoichiometry and turnover in single, functioning membrane protein complexes. Nature 443(7109):355–358. https://doi.org/10.1038/nature05135

Lee J, Monzingo AF, Keatinge-Clay AT, Harshey RM (2015) Structure of *Salmonella* FlhE, conserved member of a flagellar type III secretion operon. J Mol Biol 427(6):1254–1262. https://doi.org/10.1016/j.jmb.2014.11.022

Lele PP, Branch RW, Nathan VS, Berg HC (2012) Mechanism for adaptive remodeling of the bacterial flagellar switch. Proc Natl Acad Sci USA 109(49):20018–20022. https://doi.org/10.1073/pnas.1212327109

Lele PP, Hosu BG, Berg HC (2013) Dynamics of mechanosensing in the bacterial flagellar motor. Proc Natl Acad Sci USA 110(29):11839–11844. https://doi.org/10.1073/pnas.1305885110

Levenson R, Zhou H, Dahlquist FW (2012) Structural insights into the interaction between the bacterial flagellar motor proteins FliF and FliG. Biochemistry 51(25):5052–5060. https://doi.org/10.1021/bi3004582

Macnab RM (2003) How bacteria assemble flagella. Annu Rev Microbiol 57:77–100. https://doi.org/10.1146/annurev.micro.57.030502.090832

Maki-Yonekura S, Yonekura K, Namba K (2003) Domain movements of HAP2 in the cap-filament complex formation and growth process of the bacterial flagellum. Proc Natl Acad Sci USA 100(26):15528–15533. https://doi.org/10.1073/pnas.2534343100

Maki-Yonekura S, Yonekura K, Namba K (2010) Conformational change of flagellin for polymorphic supercoiling of the flagellar filament. Nat Struct Mol Biol 17(4):417–422. https://doi.org/10.1038/nsmb.1774

Manson MD, Tedesco P, Berg HC, Harold FM, Van der Drift C (1977) A protonmotive force drives bacterial flagella. Proc Natl Acad Sci USA 74(7):3060–3064. https://doi.org/10.1073/pnas.74.7.3060

Minamino T (2014) Protein export through the bacterial flagellar type III export pathway. Biochim Biophys Acta 1843(8):1642–1648. https://doi.org/10.1016/j.bbamcr.2013.09.005

Minamino T (2018) Hierarchical protein export mechanism of the bacterial flagellar type III protein export apparatus. FEMS Microbiol Lett 365(12):fny117. https://doi.org/10.1093/femsle/fny117

Minamino T, Namba K (2008) Distinct roles of the FliI ATPase and proton motive force in bacterial flagellar protein export. Nature 451(7177):485–488. https://doi.org/10.1038/nature06449

Minamino T, Macnab RM (2000a) Domain structure of *Salmonella* FlhB, a flagellar export component responsible for substrate specificity switching. J Bacteriol 182(17):4906–4914. https://doi.org/10.1128/jb.182.17.4906-4914.2000

Minamino T, Macnab RM (2000b) Interactions among components of the *Salmonella* flagellar export apparatus and its substrates. Mol Microbiol 35(5):1052–1064. https://doi.org/10.1046/j.1365-2958.2000.01771.x

Minamino T, Imada K (2015) The bacterial flagellar motor and its structural diversity. Trends Microbiol 23(5):267–274. https://doi.org/10.1016/j.tim.2014.12.011

Minamino T, Iino T, Kutuskake K (1994) Molecular characterization of the *Salmonella typhimurium flhB* operon and its protein products. J Bacteriol 176(24):7630–7637. https://doi.org/10.1128/jb.176.24.7630-7637.1994

Minamino T, Yamaguchi S, Macnab RM (2000) Interaction between FliE and FlgB, a proximal rod component of the flagellar basal body of *Salmonella.* J Bacteriol 182(11):3029–3036. https://doi.org/10.1128/jb.182.11.3029-3036.2000

Minamino T, Kazetani KI, Tahara A, Suzuki H, Furukawa Y, Kihara M, Namba K (2006) Oligomerization of the bacterial flagellar ATPase FliI is controlled by its extreme N-terminal region. J Mol Biol 360(2):510–519. https://doi.org/10.1016/j.jmb.2006.05.010

Minamino T, Yoshimura SD, Morimoto YV, Gonzalez-Pedrajo B, Kami-Ike N, Namba K (2009) Roles of the extreme N-terminal region of FliH for efficient localization of the FliH-FliI complex to the bacterial flagellar type III export apparatus. Mol Microbiol 74(6):1471–1483. https://doi.org/10.1111/j.1365-2958.2009.06946.x

Minamino T, Imada K, Namba K (2008) Molecular motors of the bacterial flagella. Curr Opin Struct Biol 18(6):693–701. https://doi.org/10.1016/j.sbi.2008.09.006

Minamino T, Shimada M, Okabe M, Saijo-Hamano Y, Imada K, Kihara M, Namba K (2010) Role of the C-terminal cytoplasmic domain of FlhA in bacterial flagellar type III protein export. J Bacteriol 192(7):1929–1936. https://doi.org/10.1128/JB.01328-09

Minamino T, Imada K, Kinoshita M, Nakamura S, Morimoto YV, Namba K (2011a) Structural insight into the rotational switching mechanism of the bacterial flagellar motor. PLoS Biol 9(5):12. https://doi.org/10.1371/journal.pbio.1000616

Minamino T, Morimoto YV, Hara N, Namba K (2011b) An energy transduction mechanism used in bacterial flagellar type III protein export. Nat Commun 2:475. https://doi.org/10.1038/ncomms1488

Minamino T, Kinoshita M, Hara N, Takeuchi S, Hida A, Koya S, Glenwright H, Imada K, Aldridge PD, Namba K (2012) Interaction of a bacterial flagellar chaperone FlgN with FlhA is required for efficient export of its cognate substrates. Mol Microbiol 83(4):775–788. https://doi.org/10.1111/j.1365-2958.2011.07964.x

Minamino T, Kinoshita M, Inoue Y, Morimoto YV, Ihara K, Koya S, Hara N, Nishioka N, Kojima S, Homma M, Namba K (2016a) FliH and FliI ensure efficient energy coupling of flagellar type III protein export in *Salmonella.* Microbiologyopen 5(3):424–435. https://doi.org/10.1002/mbo3.340

Minamino T, Morimoto YV, Hara N, Aldridge PD, Namba K (2016b) The bacterial flagellar type III export gate complex is a dual fuel engine that can use both H^+ and Na^+ for flagellar protein export. PLoS Pathog 12(3):e1005495. https://doi.org/10.1371/journal.ppat.1005495

Minamino T, Terahara N, Kojima S, Namba K (2018) Autonomous control mechanism of stator assembly in the bacterial flagellar motor in response to changes in the environment. Mol Microbiol 109(6):723–734. https://doi.org/10.1111/mmi.14092

Minamino T, Kawamoto A, Kinoshita M, Namba K (2020a) Molecular organization and assembly of the export apparatus of flagellar type III secretion systems. Curr Top Microbiol Immunol. 427: 91–107. https://doi.org/10.1007/82_2019_170

Minamino T, Inoue Y, Kinoshita M, Namba K (2020b) FliK-driven conformational rearrangements of FlhA and FlhB are required for export switching of the flagellar protein export apparatus. J Bacteriol 202(3): e00637-19. https://doi.org/10.1128/JB.00637-19

Miyanoiri Y, Hijikata A, Nishino Y, Gohara M, Onoue Y, Kojima S, Kojima C, Shirai T, Kainosho M, Homma M (2017) Structural and functional analysis of the C-terminal region of FliG, an essential motor component of *Vibrio* Na^+-driven flagella. Structure 25(10):1540–1548, e1543. https://doi.org/10.1016/j.str.2017.08.010

Morimoto YV, Minamino T (2014) Structure and function of the bi-directional bacterial flagellar motor. Biomolecules 4(1):217–234. https://doi.org/10.3390/biom4010217

Morimoto YV, Che YS, Minamino T, Namba K (2010a) Proton-conductivity assay of plugged and unplugged MotA/B proton channel by cytoplasmic pHluorin expressed in *Salmonella*. FEBS Lett 584(6):1268–1272. https://doi.org/10.1016/j.febslet.2010.02.051

Morimoto YV, Nakamura S, Kami-ike N, Namba K, Minamino T (2010b) Charged residues in the cytoplasmic loop of MotA are required for stator assembly into the bacterial flagellar motor. Mol Microbiol 78(5):1117–1129. https://doi.org/10.1111/j.1365-2958.2010.07391.x

Morimoto YV, Nakamura S, Hiraoka KD, Namba K, Minamino T (2013) Distinct roles of highly conserved charged residues at the MotA-FliG interface in bacterial flagellar motor rotation. J Bacteriol 195(3):474–481. https://doi.org/10.1128/JB.01971-12

Morimoto YV, Ito M, Hiraoka KD, Che YS, Bai F, Kami-Ike N, Namba K, Minamino T (2014) Assembly and stoichiometry of FliF and FlhA in *Salmonella* flagellar basal body. Mol Microbiol 91(6):1214–1226. https://doi.org/10.1111/mmi.12529

Morimoto YV, Kami-Ike N, Miyata T, Kawamoto A, Kato T, Namba K, Minamino T (2016) High-resolution pH imaging of living bacterial cells to detect local pH differences. mBio 7(6). https://doi.org/10.1128/mBio.01911-16

Muramoto K, Macnab RM (1998) Deletion analysis of MotA and MotB, components of the force-generating unit in the flagellar motor of *Salmonella.* Mol Microbiol 29(5):1191–1202. https://doi.org/10.1046/j.1365-2958.1998.00998.x

Muskotal A, Seregelyes C, Sebestyen A, Vonderviszt F (2010) Structural basis for stabilization of the hypervariable D3 domain of *Salmonella* flagellin upon filament formation. J Mol Biol 403(4):607–615. https://doi.org/10.1016/j.jmb.2010.09.024

Nakamura S, Minamino T (2019) Flagella-driven motility of bacteria. Biomolecules 9(7):279. https://doi.org/10.3390/biom9070279

Nakamura S, Hanaizumi Y, Morimoto YV, Inoue Y, Erhardt M, Minamino T, Namba K (2019) Direct observation of speed fluctuations of flagellar motor rotation at extremely low load close to zero. Mol Microbiol 113 vhttps://doi.org/10.1111/mmi.14440

Namba K, Vonderviszt F (1997) Molecular architecture of bacterial flagellum. Q Rev Biophys 30(1):1–65. https://doi.org/10.1017/s0033583596003319

Okabe M, Minamino T, Imada K, Namba K, Kihara M (2009) Role of the N-terminal domain of FliI ATPase in bacterial flagellar protein export. FEBS Lett 583(4):743–748. https://doi.org/10.1016/j.febslet.2009.01.026

Paul K, Gonzalez-Bonet G, Bilwes AM, Crane BR, Blair D (2011) Architecture of the flagellar rotor. EMBO J 30(14):2962–2971. https://doi.org/10.1038/emboj.2011.188

Paul K, Erhardt M, Hirano T, Blair DF, Hughes KT (2008) Energy source of flagellar type III secretion. Nature 451(7177):489–492. https://doi.org/10.1038/nature06497

Paul K, Nieto V, Carlquist WC, Blair DF, Harshey RM (2010) The c-di-GMP binding protein YcgR controls flagellar motor direction and speed to affect chemotaxis by a "backstop brake" mechanism. Mol Cell 38(1):128–139. https://doi.org/10.1016/j.molcel.2010.03.001

Postel S, Deredge D, Bonsor DA, Yu X, Diederichs K, Helmsing S, Vromen A, Friedler A, Hust M, Egelman EH, Beckett D, Wintrode PL, Sundberg EJ (2016) Bacterial flagellar capping proteins adopt diverse oligomeric states. eLife 5:e18857. https://doi.org/10.7554/eLife.18857

Pourjaberi SNS, Terahara N, Namba K, Minamino T (2017) The role of a cytoplasmic loop of MotA in load-dependent assembly and disassembly dynamics of the MotA/B stator complex in the bacterial flagellar motor. Mol Microbiol 106(4):646–658. https://doi.org/10.1111/mmi.13843

Ravid S, Eisenbach M (1984) Minimal requirements for rotation of bacterial flagella. J Bacteriol 158(3):1208–1210

Reid SW, Leake MC, Chandler JH, Lo CJ, Armitage JP, Berry RM (2006) The maximum number of torque-generating units in the flagellar motor of *Escherichia coli* is at least 11. Proc Natl Acad Sci USA 103(21):8066–8071. https://doi.org/10.1073/pnas.0509932103

Saijo-Hamano Y, Uchida N, Namba K, Oosawa K (2004) In vitro characterization of FlgB, FlgC, FlgF, FlgG, and FliE, flagellar basal body proteins of *Salmonella.* J Mol Biol 339(2):423–435. https://doi.org/10.1016/j.jmb.2004.03.070

Saijo-Hamano Y, Matsunami H, Namba K, Imada K (2019) Architecture of the Bacterial Flagellar Distal Rod and Hook of *Salmonella*. Biomolecules 9(7):260. https://doi.org/10.3390/biom9070260

Sakai T, Inoue Y, Terahara N, Namba K, Minamino T (2018) A triangular loop of domain D1 of FlgE is essential for hook assembly but not for the mechanical function. Biochem Biophys Res Commun 495(2):1789–1794. https://doi.org/10.1016/j.bbrc.2017.12.037

Sakai T, Miyata T, Terahara N, Mori K, Inoue Y, Morimoto YV, Kato T, Namba K, Minamino T (2019) Novel insights into conformational rearrangements of the bacterial flagellar switch complex. mBio 10(2):e00079–19. https://doi.org/10.1128/mBio.00079-19

Samatey FA, Imada K, Nagashima S, Vonderviszt F, Kumasaka T, Yamamoto M, Namba K (2001) Structure of the bacterial flagellar protofilament and implications for a switch for supercoiling. Nature 410(6826):331–337. https://doi.org/10.1038/35066504

Samatey FA, Matsunami H, Imada K, Nagashima S, Shaikh TR, Thomas DR, Chen JZ, Derosier DJ, Kitao A, Namba K (2004) Structure of the bacterial flagellar hook and implication for the molecular universal joint mechanism. Nature 431(7012):1062–1068. https://doi.org/10.1038/nature02997

Sarkar MK, Paul K, Blair D (2010) Chemotaxis signaling protein CheY binds to the rotor protein FliN to control the direction of flagellar rotation in *Escherichia coli*. Proc Natl Acad Sci USA 107(20):9370–9375. https://doi.org/10.1073/pnas.1000935107

Shibata S, Matsunami H, Aizawa SI, Wolf M (2019) Torque transmission mechanism of the curved bacterial flagellar hook revealed by cryo-EM. Nat Struct Mol Biol 26(10):941–945. https://doi.org/10.1038/s41594-019-0301-3

Song WS, Cho SY, Hong HJ, Park SC, Yoon SI (2017) Self-oligomerizing structure of the flagellarcap protein FliD and its implication in filament assembly. J Mol Biol 429(6):847–857. https://doi.org/10.1016/j.jmb.2017.02.001

Stocker BAD (1949) Measurement of the rate of mutation of flagellar antigenic phase in *Salmonella* typhimurium. J Hyg 47:398–413

Suzuki H, Yonekura K, Namba K (2004) Structure of the rotor of the bacterial flagellar motor revealed by electron cryomicroscopy and single-particle image analysis. J Mol Biol 337(1):105–113. https://doi.org/10.1016/j.jmb.2004.01.034

Suzuki Y, Morimoto YV, Oono K, Hayashi F, Oosawa K, Kudo S, Nakamura S (2019) Effect of the MotA(M206I) mutation on torque generation and stator assembly in the *Salmonella* H^+-driven flagellar motor. J Bacteriol 201(6):e00727-e818. https://doi.org/10.1128/JB.00727-18

Takekawa N, Terahara N, Kato T, Gohara M, Mayanagi K, Hijikata A, Onoue Y, Kojima S, Shirai T, Namba K, Homma M (2016) The tetrameric MotA complex as the core of the flagellar motor stator from hyperthermophilic bacterium. Sci Rep 6:31526. https://doi.org/10.1038/srep31526

Terahara N, Kodera N, Uchihashi T, Ando T, Namba K, Minamino T (2017a) Na^+-induced structural transition of MotPS for stator assembly of the *Bacillus* flagellar motor. Sci Adv 3(11):eaao4119. https://doi.org/10.1126/sciadv.aao4119

Terahara N, Noguchi Y, Nakamura S, Kami-Ike N, Ito M, Namba K, Minamino T (2017b) Load- and polysaccharide-dependent activation of the Na^+-type MotPS stator in the *Bacillus subtilis* flagellar motor. Sci Rep 7:46081. https://doi.org/10.1038/srep46081

Terahara N, Inoue Y, Kodera N, Morimoto YV, Uchihashi T, Imada K, Ando T, Namba K, Minamino T (2018) Insight into structural remodeling of the FlhA ring responsible for bacterial flagellar type III protein export. Sci Adv 4(4):eaao7054. https://doi.org/10.1126/sciadv.aao7054

Thomas J, Stafford GP, Hughes C (2004) Docking of cytosolic chaperone-substrate complexes at the membrane ATPase during flagellar type III protein export. Proc Natl Acad Sci USA 101(11):3945–3950. https://doi.org/10.1073/pnas.0307223101

Tipping MJ, Delalez NJ, Lim R, Berry RM, Armitage JP (2013) Load-dependent assembly of the bacterial flagellar motor. mBio 4(4). https://doi.org/10.1128/mBio.00551-13

Ueno T, Oosawa K, Aizawa S (1992) M ring, S ring and proximal rod of the flagellar basal body of Salmonella typhimurium are composed of subunits of a single protein, FliF. J Mol Biol 227(3):672–677. https://doi.org/10.1016/0022-2836(92)90216-7

Vartanian AS, Paz A, Fortgang EA, Abramson J, Dahlquist FW (2012) Structure of flagellar motor proteins in complex allows for insights into motor structure and switching. J Biol Chem 287(43):35779–35783. https://doi.org/10.1074/jbc.C112.378380

Yamaguchi S, Aizawa S, Kihara M, Isomura M, Jones CJ, Macnab RM (1986) Genetic evidence for a switching and energy-transducing complex in the flagellar motor of *Salmonella typhimurium*. J Bacteriol 168(3):1172–1179. https://doi.org/10.1128/jb.168.3.1172-1179.1986

Yamaguchi T, Toma S, Terahara N, Miyata T, Ashihara M, Minamino T, Namba K, Kato T (2020) Structural and functional comparison of *Salmonella* flagellar filaments composed of FljB and FliC. Biomolecules 10(2):246. https://doi.org/10.3390/biom10020246

Yonekura K, Maki S, Morgan DG, DeRosier DJ, Vonderviszt F, Imada K, Namba K (2000) The bacterial flagellar cap as the rotary promoter of flagellin self-assembly. Science 290(5499):2148–2152. https://doi.org/10.1126/science.290.5499.2148

Yonekura K, Maki-Yonekura S, Namba K (2003) Complete atomic model of the bacterial flagellar filament by electron cryomicroscopy. Nature 424(6949):643–650. https://doi.org/10.1038/nature01830

Yuan J, Berg HC (2008) Resurrection of the flagellar rotary motor near zero load. Proc Natl Acad Sci USA 105(4):1182–1185. https://doi.org/10.1073/pnas.0711539105

Zhou J, Fazzio RT, Blair DF (1995) Membrane topology of the MotA protein of *Escherichia coli*. J Mol Biol 251(2):237–242. https://doi.org/10.1006/jmbi.1995.0431

Zhou J, Lloyd SA, Blair DF (1998a) Electrostatic interactions between rotor and stator in the bacterial flagellar motor. Proc Natl Acad Sci USA 95(11):6436–6441. https://doi.org/10.1073/pnas.95.11.6436

Zhou J, Sharp LL, Tang HL, Lloyd SA, Billings S, Braun TF, Blair DF (1998b) Function of protonatable residues in the flagellar motor of *Escherichia coli*: a critical role for Asp 32 of MotB. J Bacteriol 180(10):2729–2735